Nature of Prominences and their role in Space Weather
Proceedings IAU Symposium No. 300, 2013
B. Schmieder, J.-M. Malherbe & S. T. Wu, eds.

doi:10.1017/S1743921313011083

Reconstruction of magnetic clouds from in-situ spacecraft measurements and intercomparison with their solar sources

Qiang Hu[1] and Jiong Qiu[2]

[1]Dept. of Space Science/CSPAR, University of Alabama in Huntsville, Huntsville, AL 35805, USA
email: qh0001@uah.edu

[2]Physics Department, Montana State University, Bozeman, MT 59717-3840, USA
email: qiuj@mithra.physics.montana.edu

Abstract. Coronal Mass Ejections (CMEs) are eruptive events that originate, propagate away from the Sun, and carry along solar material with embedded solar magnetic field. Some are accompanied by prominence eruptions. A subset of the interplanetary counterparts of CMEs (ICMEs), so-called Magnetic Clouds (MCs) can be characterized by magnetic flux-rope structures. We apply the Grad-Shafranov (GS) reconstruction technique to examine the configuration of MCs and to derive relevant physical quantities, such as magnetic flux content, relative magnetic helicity, and the field-line twist, etc. Both observational analyses of solar source region characteristics including flaring and associated magnetic reconnection process, and the corresponding MC structures were carried out. We summarize the main properties of selected events with and without associated prominence eruptions. In particular, we show the field-line twist distribution and the intercomparison of magnetic flux for these flux-rope structures.

Keywords. Magnetic Clouds, Magnetic Flux Rope, CME/ICME, In Situ Measurements, Prominence

1. Introduction

This report addresses the magnetic field topology of Magnetic Clouds (MCs) and the connection to their solar sources. We focus on the quantitative characterization of MC/flux-rope structures at 1 AU, and illustrate our approach to inter-connecting the solar and interplanetary analysis. We treat the magnetic structure of prominence as an integral part of the MC observed in-situ (Schmieder *et al.* 2013; van Ballegooijen & Martens 1989). We note that all events examined here were associated with solar flares. Some were accompanied by prominence eruption (PE) and others were not (non-PE), according to Li (2012) and our own assessment.

2. Grad-Shafranov Reconstruction of Magnetic Clouds

Magnetic Clouds are a subset of ICMEs that possess the following characteristics based on in-situ spacecraft measurements (e.g., Burlaga 1995): 1) relatively strong magnetic field, 2) smooth rotation of the magnetic field direction, and 3) relatively low proton temperature or proton β value. This is a traditional definition and has enabled the modeling of such structures via traditional force-free approaches (Burlaga 1995). An alternative and now widely used approach, beyond the force-free assumption, is based on the plane Grad-Shafranov equation that allows the analysis of events that are not strictly

MCs. For example, when electron temperature is included, the total plasma pressure can be significantly increased, resulting in total plasma β values $\geqslant 1$ where the GS method is still applicable (Hu *et al.* 2013). Overall all approaches have yielded flux-rope solutions for the structures embedded within MC or ICME intervals. A typical output of a GS reconstruction result is shown in Fig. 1.

Here a typical cylindrical flux-rope configuration is illustrated by three selected thick spiral field lines, lying on nested isosurfaces of the magnetic flux function A whose projection onto the $x-y$ plane is shown in the back as equi-value contours of A. The flux rope axis along z represents the invariance direction (i.e., $\partial/\partial z = 0$, and $B_z = B_z(A)$). Various physical quantities can be derived based on the GS reconstruction result. For example, the total toroidal (axial) magnetic flux $\Phi_t = \int B_z dxdy$ and the total poloidal magnetic flux $\Phi_p = |A_0 - A_b| \cdot L$, i.e., the flux across the shaded area in Fig. 1, for certain effective length L along z. Correspondingly, the relative magnetic helicity within certain volume can be calculated (Webb *et al.* 2010). Additionally the axial magnetic field and electric current density distributions, the accumulative and total current etc. can also be obtained. In particular, we derive the field-line twist as a function of A to examine its variation within the flux rope. A highly relevant study was carried out by Dasso *et al.* (2006) where four different analytic flux-rope models were employed to derive various physical quantities for one event.

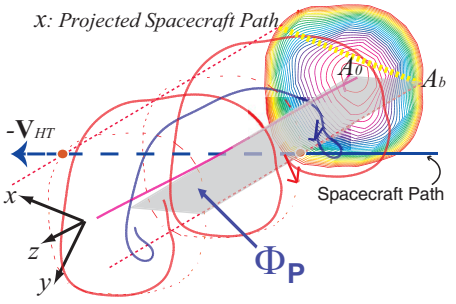

Figure 1. A typical GS reconstruction result of a cylindrical magnetic flux rope. See text for details.

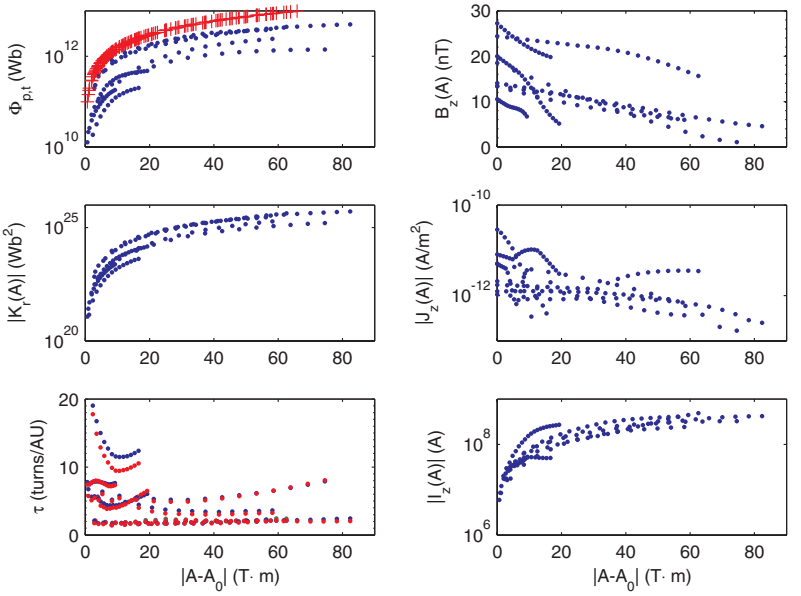

Figure 2. Summary plot of various quantities as functions of A for selected events (Li 2012). (*from top to bottom*) Left column: toroidal and poloidal ('+') flux, relative magnetic helicity, and field-line twist; right column: axial magnetic field, axial current density, and accumulative axial current.

https://doi.org/10.1017/S1743921313011083 Published online by Cambridge University Press

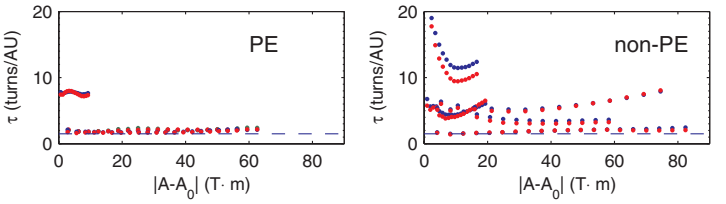

Figure 3. Field-line twist for PE (*left*) and non-PE (*right*) events. The horizontal dashed line is of value 1.5.

Fig. 2 shows the summary plot of various quantities for a handful of events, especially as organized by the shifted flux function A, which represents different cylindrical shells of varying radial distance away from the center ($A \equiv A_0$) of the flux rope, the larger the shifted A values, the farther the distances away from the center. Generally speaking, the maximum A value indicates the transverse size of each flux rope. The distributions of $B_z(A)$ and $|J_z(A)|$ show greater ranges of variation, while the integral quantities of magnetic flux, electric current and relative magnetic helicity do not. They all increase monotonically, and they do not appear to have clear distinctions between PE and non-PE events.

The average magnetic field line twist is approximated by $\tau(A) = K_r(A)/\Phi_t^2(A)$ (Berger & Field 1984), and similarly $\tau(A) = \Phi_p(A)/\Phi_t(A)$, based on the assumption of a constant twist. Both are functions of A, representing an average twist, in terms of number of turns per AU, within the volume enclosed by each A shell. The bottom left panel of Fig. 2 shows such twist distributions of the two numbers (dots of blue and red colors, respectively) for each event. Each set of blue and red dots overlaps very well, except for the one of the largest values. The general trend is that the smaller the flux rope, the larger the twist becomes. However, for events of large sizes, the twist remains fairly constant (e.g., ~ 2 turns/AU for the largest event) throughout the A shells.

We further separate the events into two categories of PE and non-PE events, and show their twist distributions, respectively, in Fig. 3. The main distinction between the two sets is that for the PE events, the twist remains largely constant within the flux rope, while for the non-PE events, the twist shows significant variations. Some exhibit declining gradient outward from the center. The implications of such behaviors are discussed in Section 4.

3. Intercomparison of Magnetic Flux

An important approach to utilize the GS reconstruction results outlined above is to make quantitative comparison with their solar sources. Following the original study of Qiu *et al.* (2007), we augmented the original list of events and show the magnetic flux comparison among Φ_p, Φ_t, and the corresponding flare-associated magnetic reconnection flux Φ_r, in Fig. 4. The comparison indicates that $\Phi_p > \Phi_t$ and $\Phi_p \approx \Phi_r$ for $L = 1$ AU with uncertainty range $L \in [0.5, 2]$ AU, which conforms to prior result (Qiu *et al.* 2007). The caveat associated with the few low points in the right panel is that the poloidal flux was significantly underestimated due to selection of a rather short interval for the GS reconstruction (~ 2 hours as opposed to normally ~ 20 hours) in some cases. There are generally no clear distinctions between PE and non-PE events, except for the two PE events of significantly greater poloidal flux than the corresponding reconnection flux. Whether or not that indicates the significant contribution from the pre-existing flux rope (prominence) is worth pursuing.

https://doi.org/10.1017/S1743921313011083 Published online by Cambridge University Press

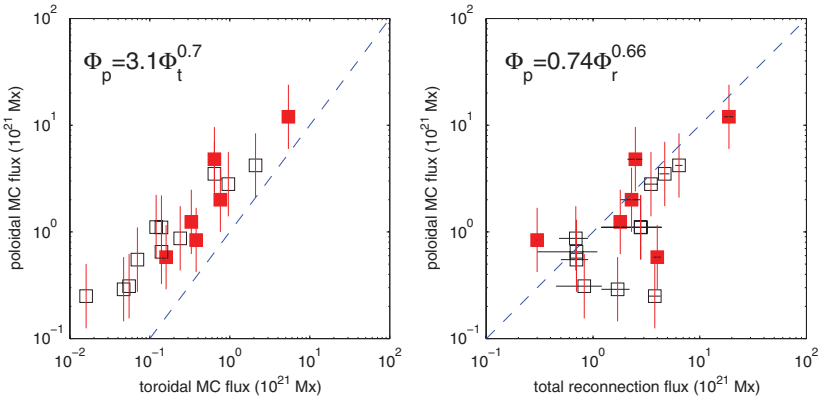

Figure 4. Magnetic flux comparison of Φ_p vs. Φ_t (*left*) and Φ_p vs. Φ_r (*right*). The events associated with PE are marked by filled squares. The least-squares fit to each data set is given and the dashed line indicates the one-to-one line.

4. Summary and Discussion

In summary, the GS reconstruction method has matured and been widely used in analyzing in-situ measurements of magnetic flux ropes. A software package has been developed and distributed world-wide for interested users. We presented the summary of the GS reconstruction results in a congregated form for a number of events, in terms of the distributions of various quantities along the A shells. Among them are the total magnetic flux ranging between 10^{11}-10^{13}Wb, the total relative helicity ranging 10^{23}-10^{26}Wb^2/AU, and the total axial current ranging 10^7-10^9A. The poloidal MC flux compares well with the magnetic reconnection flux accumulated during flare in solar source region. In addition, the non-PE (flare dominant) events showed greater gradients in field-line twist variation, especially near the flux-rope center, corresponding to the formation of flux-rope core primarily via magnetic reconnection. As a distinction for PE events (lack of strong flares), the twist distribution remains constant, which might indicate a fundamentally different formation process of the core. We plan to further elaborate on this issue and present detailed case studies elsewhere.

Acknowledgements

We acknowledge NASA grants NNG06GD41G, NNX12AF97G, and NNX12AH50G; NSF grants AGS-1062050 and ATM-0748428 for support. HQ acknowledges consultations with B. Dasgupta, A. Khare, and G.M. Webb.

References

Berger, M. A., & Field, G. B. 1984, *Journal of Fluid Mechanics*, 147, 133
Burlaga, L. 1995, *Interplanetary Magnetohydrodynamics* (New York: Oxford Univ. Press), 89
Dasso, S., Mandrini, C. H., Démoulin, P., & Luoni, M. L. 2006, *Astron. Astrophys.*, 455, 349
Hu, Q., Farrugia, C. J., Osherovich, V. A., Möstl, C., Szabo, A., Ogilvie, K. W., & Lepping, R. P. 2013, *Solar Phys.*, 284, 275
Li, Y. 2012, *private communication*
Qiu, J., Hu, Q., Howard, T. A., & Yurchyshyn, V. B. 2007, *Astrophys. J.*, 659, 758
Schmieder, B., Démoulin, P., & Aulanier, G. 2013, *Adv. Space Res.*, 51, 1967. 1212.4014
van Ballegooijen, A. A., & Martens, P. C. H. 1989, *Astrophys. J.*, 343, 971
Webb, G. M., Hu, Q., Dasgupta, B., & Zank, G. P. 2010, *J. Geophys. Res.*, 115, A10112